

Supporting Information

PdAg Nanoparticles Supported on Resorcinol-Formaldehyde Polymers Containing Amine Groups: The Promotional Effect of Phenylamine Moieties on CO₂ Transformation to Formic Acid

Shinya Masuda,^[a] Kohsuke Mori,^{*[a,b,c]} Yasutaka Kuwahara^[a,c] and Hiromi Yamashita^{*[a,c]}

^aDivision of Materials and Manufacturing Science, Graduate School of Engineering, Osaka University, 2-1 Yamadaoka, Suita, Osaka 565-0871, Japan

^bJST, PRESTO, 4-1-8 Honcho, Kawaguchi, Saitama, 332-0012, Japan

^cUnit of Elements Strategy Initiative for Catalysts Batteries (ESICB), Kyoto University, Katsura, Kyoto 615-8520, Japan

Corresponding Author

*K.M.: tel and fax, +81-6-6879-7460; e-mail, mori@mat.eng.osaka-u.ac.jp.

*H.Y.: tel and fax, +81-6-6879-7457; e-mail, yamashita@mat.eng.osaka-u.ac.jp.

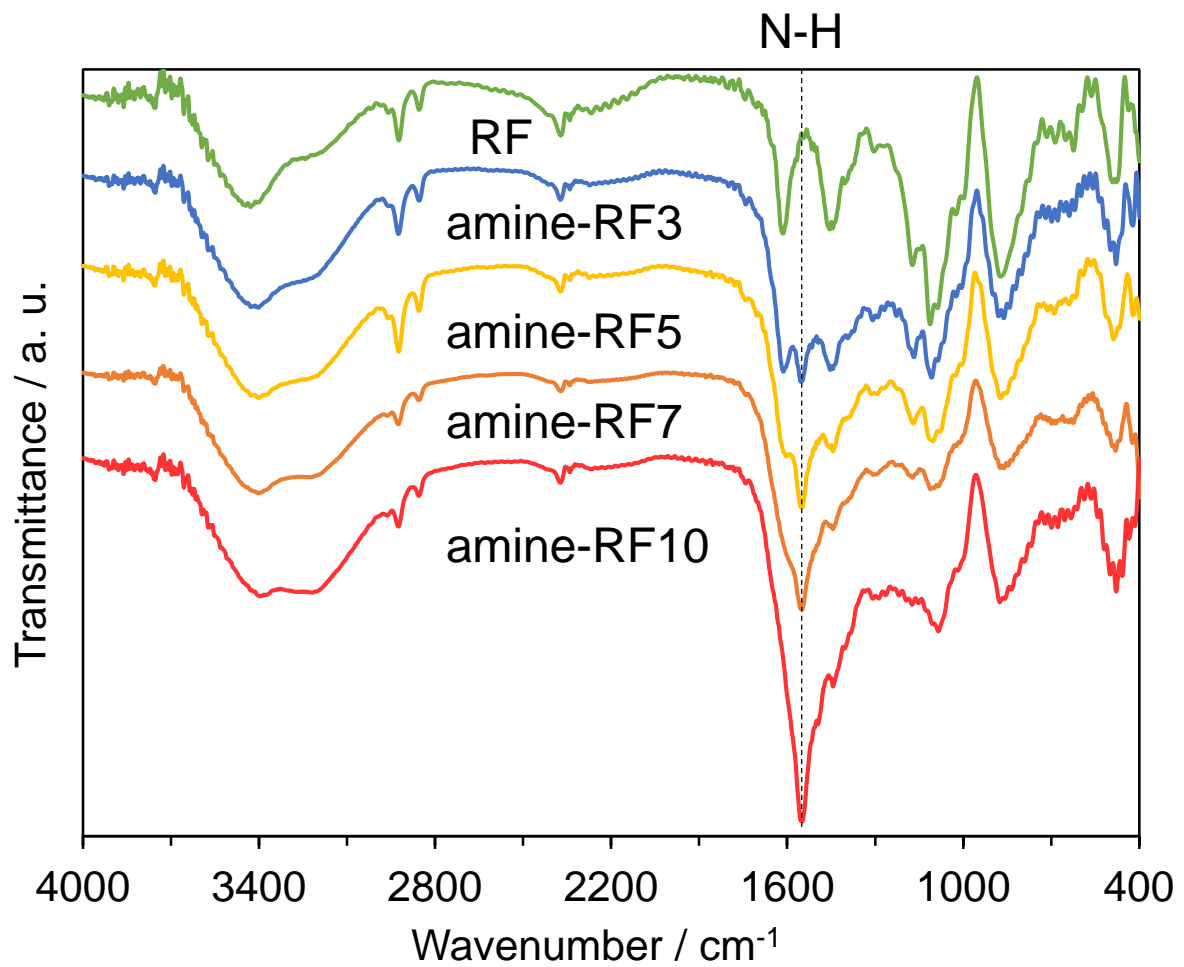


Figure S1. Fourier transform infrared spectroscopy (FT-IR) spectra of each specimens (RF, amine-RF3, amine-RF5, amine-RF7, amine-RF10).

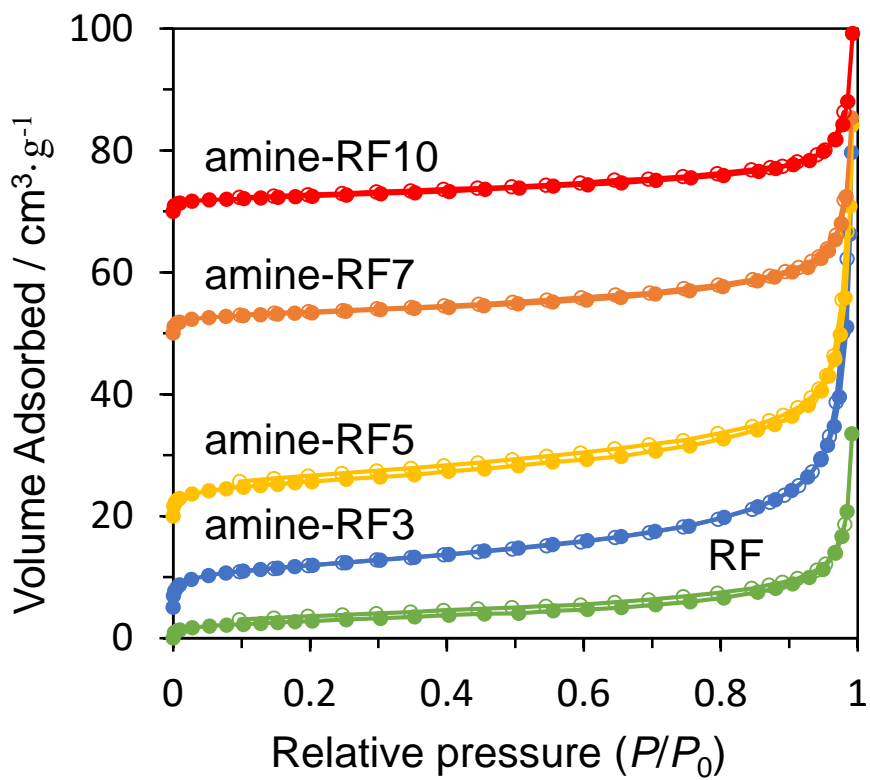


Figure S2. Nitrogen adsorption desorption isotherm of each specimens (RF, amine-RF3, amine-RF5, amine-RF7, amine-RF10).

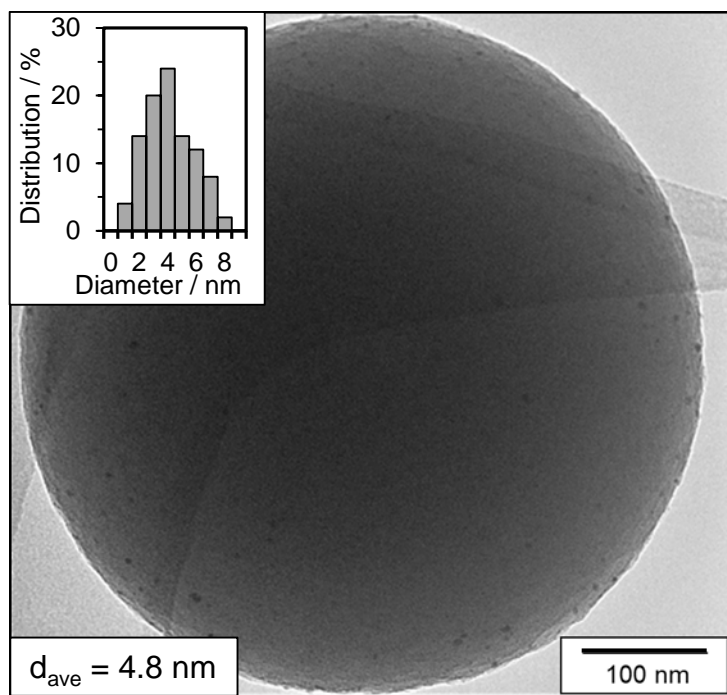


Figure S3. TEM image and size distribution diagram of PdAg NPs of PdAg/RF.

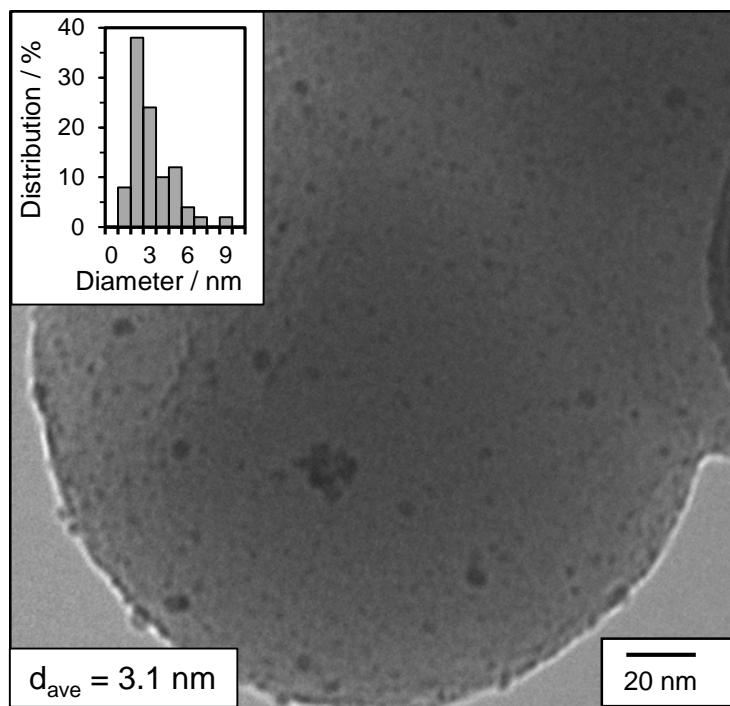


Figure S4. TEM image and size distribution diagram of PdAg NPs of PdAg/amine-RF3.

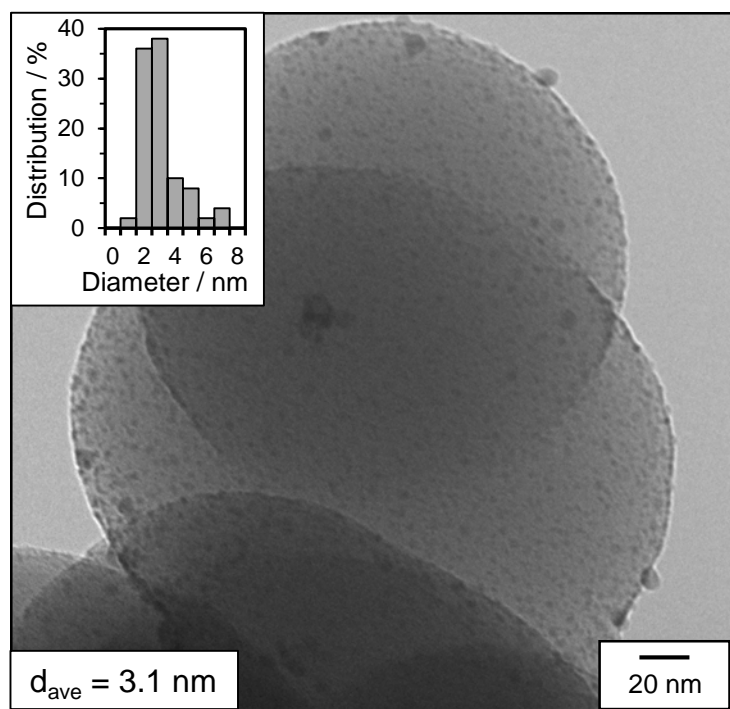


Figure S5. TEM image and size distribution diagram of PdAg NPs of PdAg/amine-RF5.

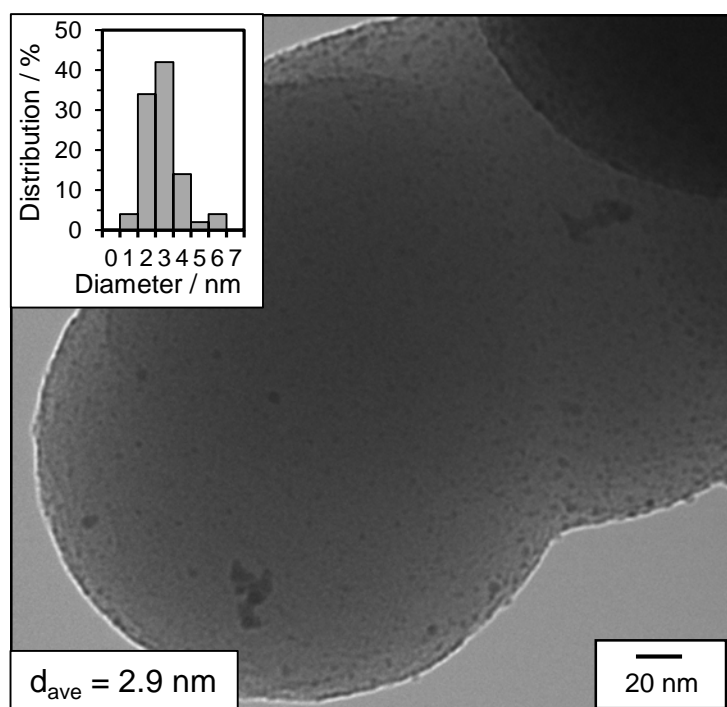


Figure S6. TEM image and size distribution diagram of PdAg NPs of PdAg/amine-RF7.

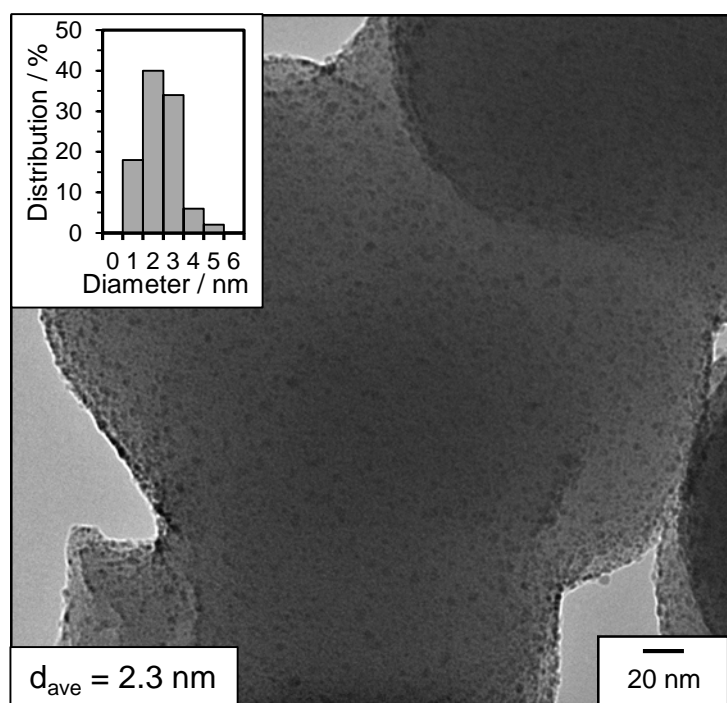


Figure S7. TEM image and size distribution diagram of PdAg NPs of PdAg/amine-RF10.

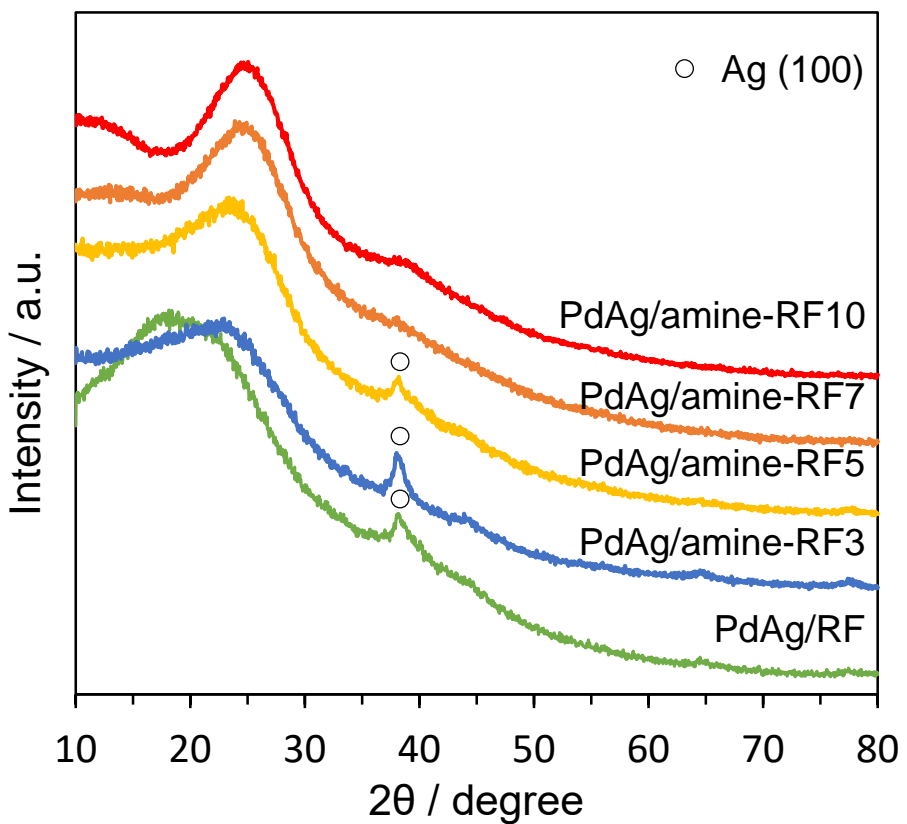


Figure S8. XRD patterns of each PdAg supported specimens (PdAg/RF, PdAg/amine-RF3, PdAg/amine-RF5, PdAg/amine-RF7, PdAg/amine-RF10).

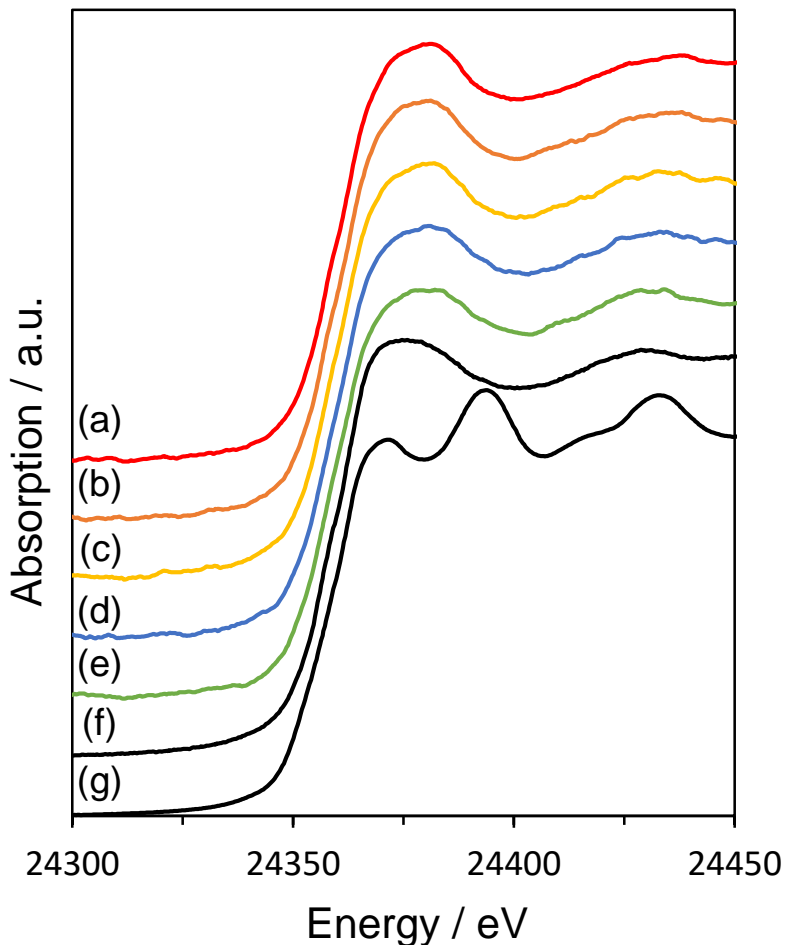


Figure S9. Pd K-edge XANES spectra of (a) PdAg/amine-RF10, (b) PdAg/amine-RF7, (c) PdAg/amine-RF5, (d) PdAg/amine-RF3, (e) PdAg/RF, (f) PdO and (g) Pd foil specimens.

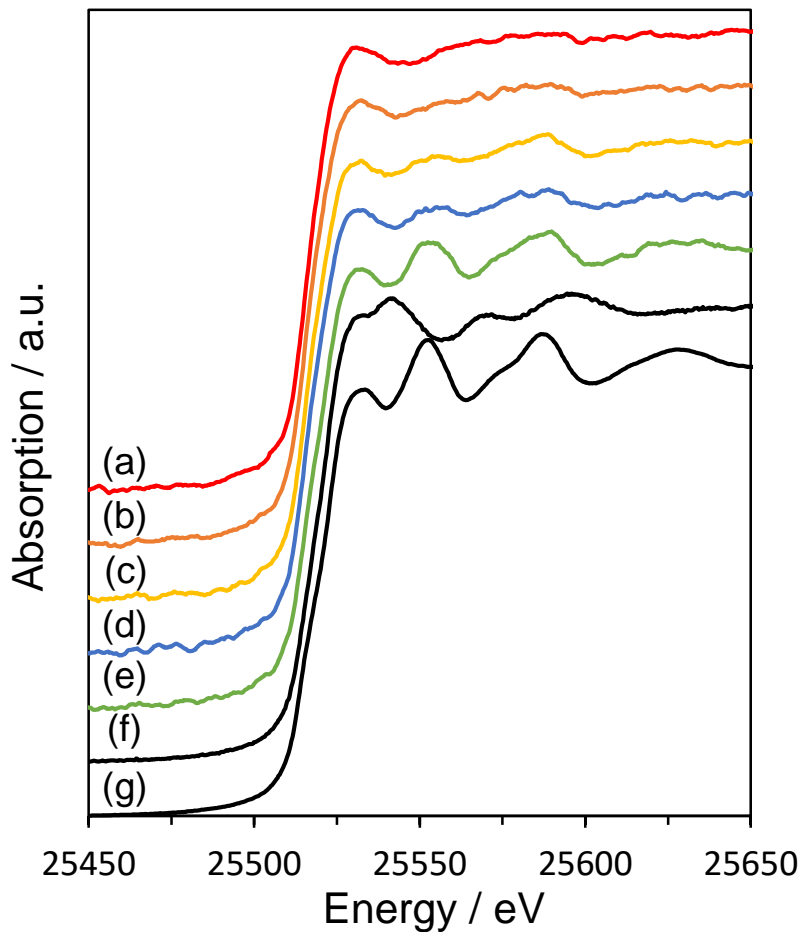


Figure S10. Ag K-edge XANES spectra of (a) PdAg/amine-RF10, (b) PdAg/amine-RF7, (c) PdAg/amine-RF5, (d) PdAg/amine-RF3, (e) PdAg/RF, (f) AgO and (g) Ag foil specimens.

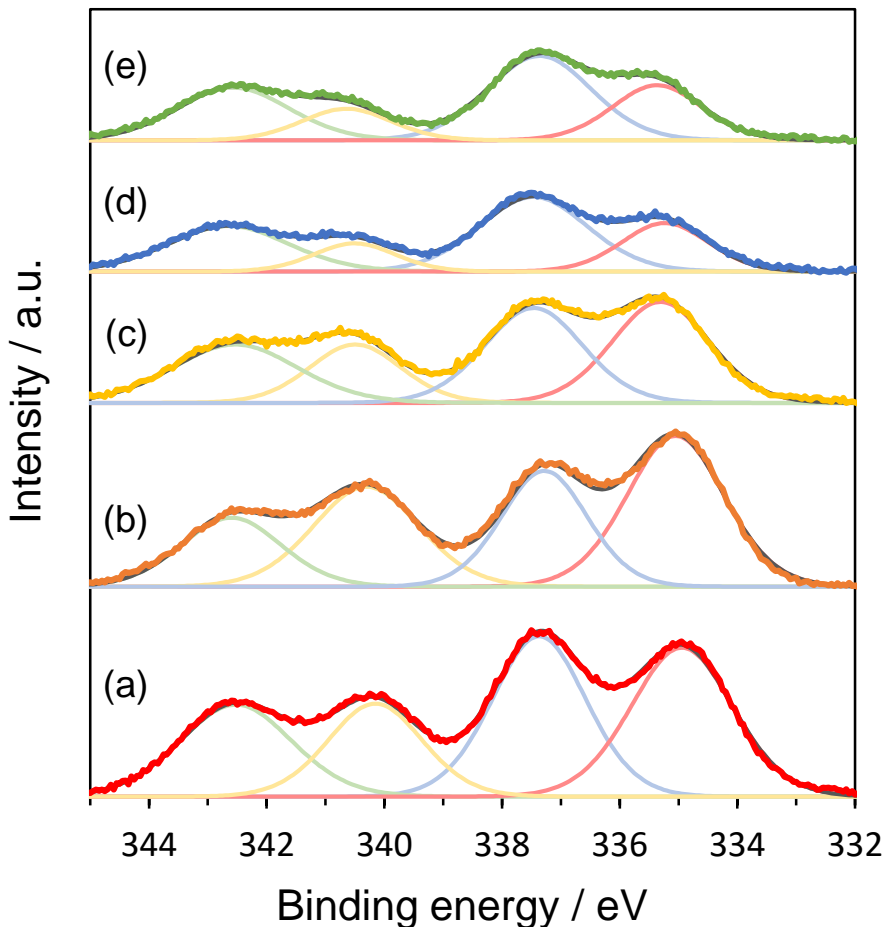


Figure S11. Pd 3d XPS spectra of (a) PdAg/amine-RF10, (b) PdAg/amine-RF7, (c) PdAg/amine-RF5 and (d) PdAg/amine-RF3, (e) PdAg/RF specimens.

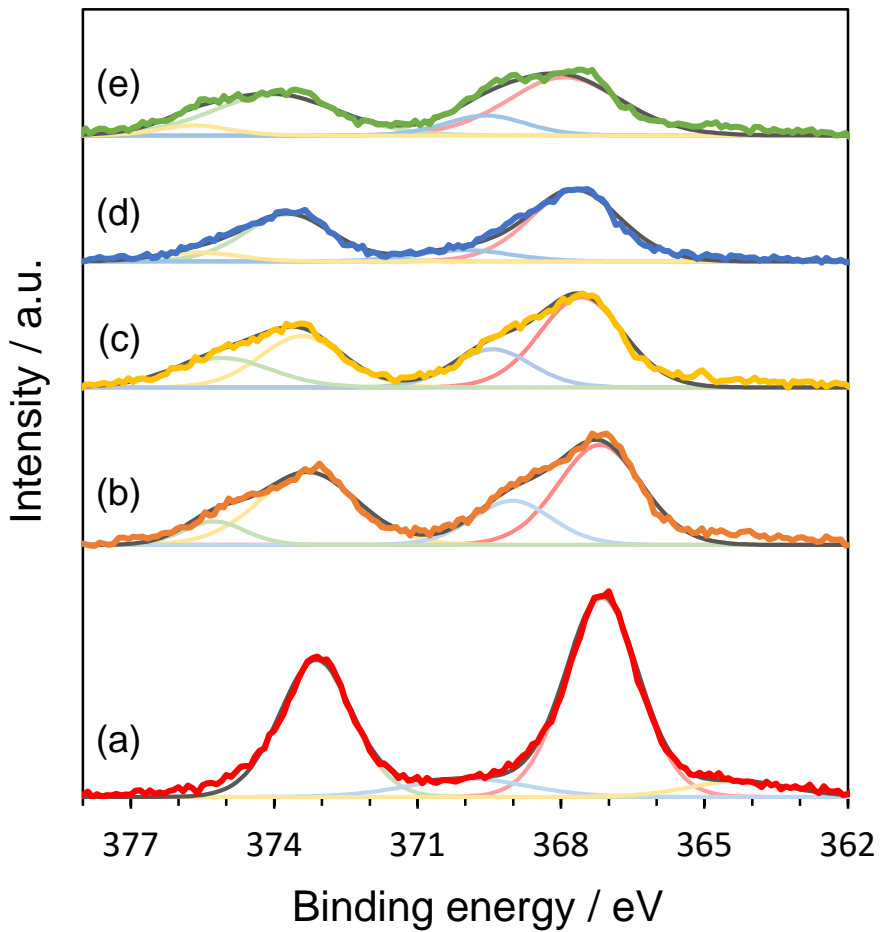


Figure S12. Ag 3d XPS spectra of (a) PdAg/amine-RF10, (b) PdAg/amine-RF7, (c) PdAg/amine-RF5 and (d) PdAg/amine-RF3, (e) PdAg/RF specimens.

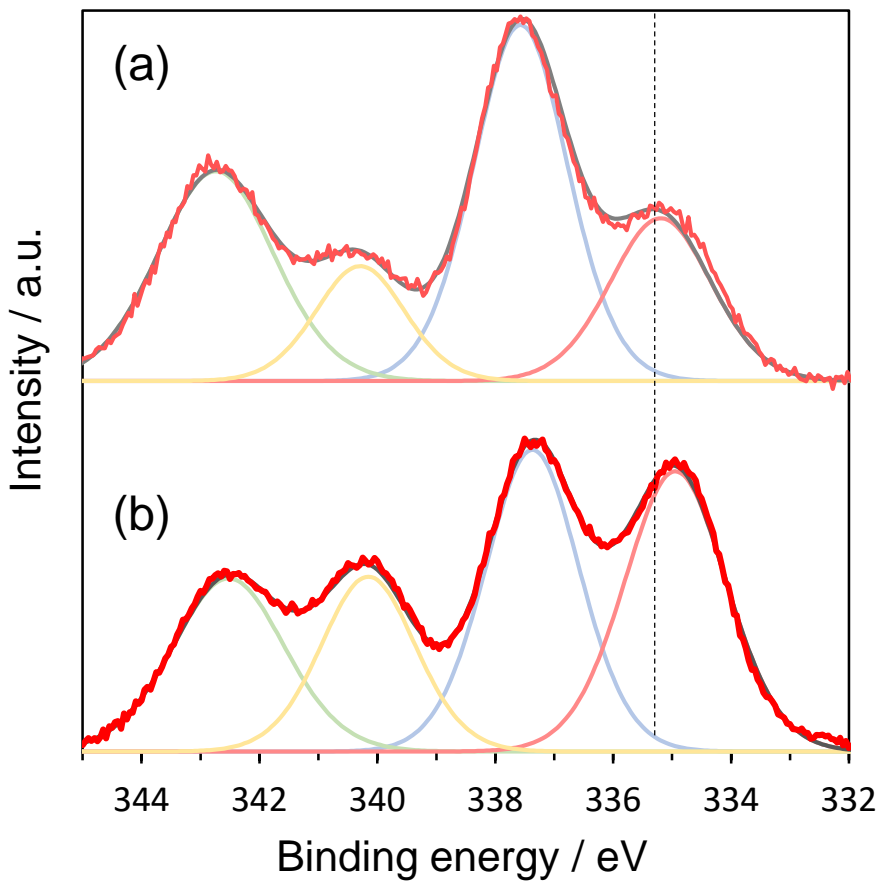


Figure S13. Pd 3d XPS spectra of (a) Pd/amine-RF10 and (b) PdAg/amine-RF10 catalysts.

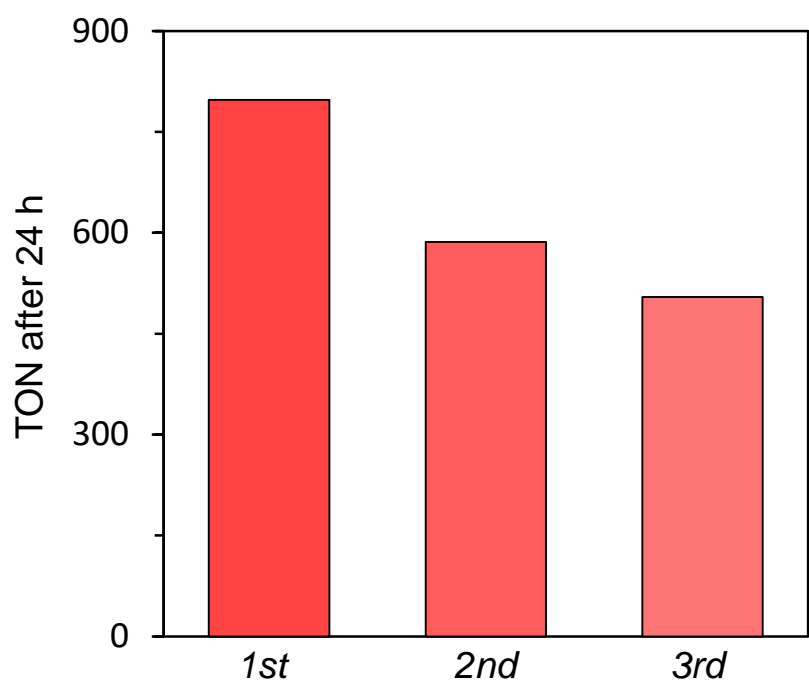


Figure S14. Recyclability of PdAg/amine-RF10 catalyst during the hydrogenation of CO₂ to produce FA. TON was calculated from total amount of loaded Pd. Reaction conditions: catalyst (10 mg), NaHCO₃ in aqueous solution (1.0 M, 15 mL) and total pressure of 2.0 MPa (CO₂:H₂ = 1:1, volume ratio) at 100 ° C for 24 h.

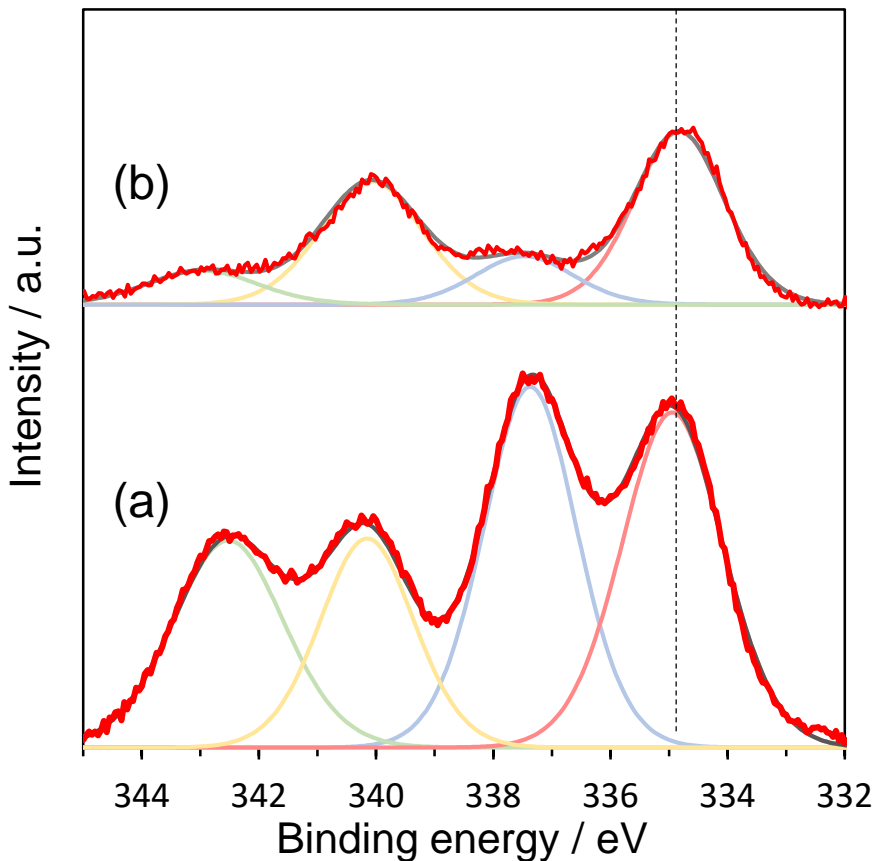


Figure S15. Difference of Pd 3d XPS spectra of (a) fresh and (b) used PdAg/amine-RF10 catalysts.

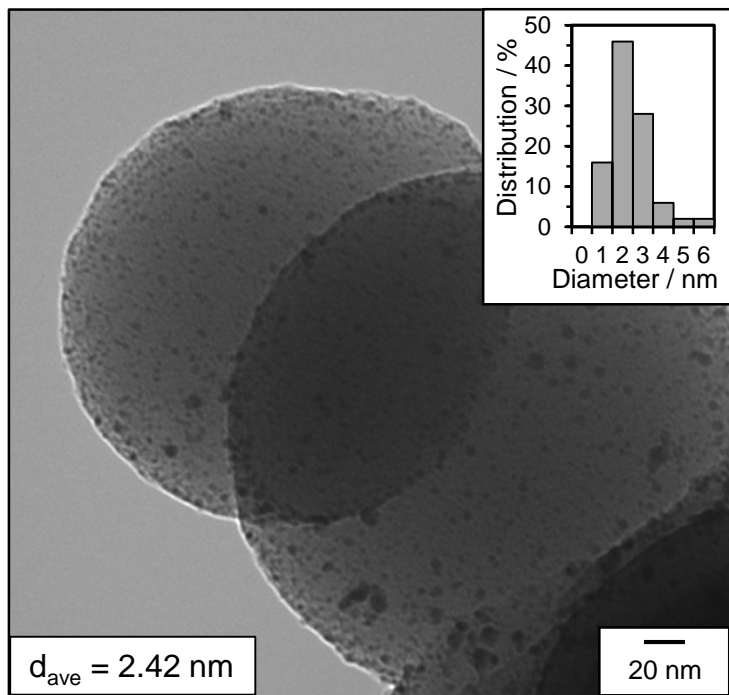


Figure S16. TEM image and size distribution diagram of PdAg NPs of PdAg/amine-RF10 after the catalytic test.

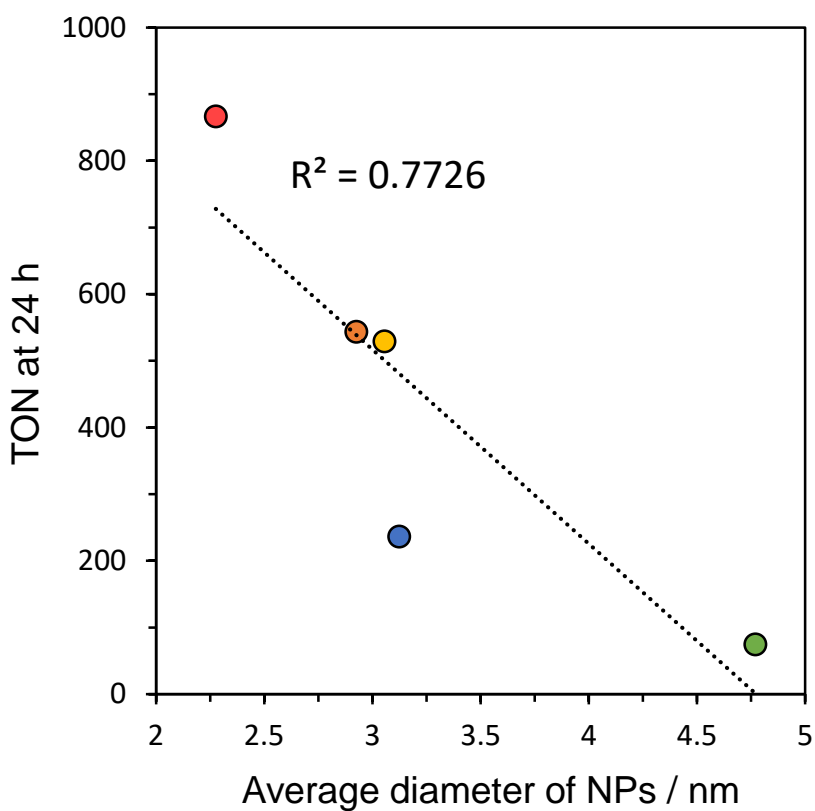


Figure S17. The relationship between TON values and average particle size calculated from TEM images of each catalysts.

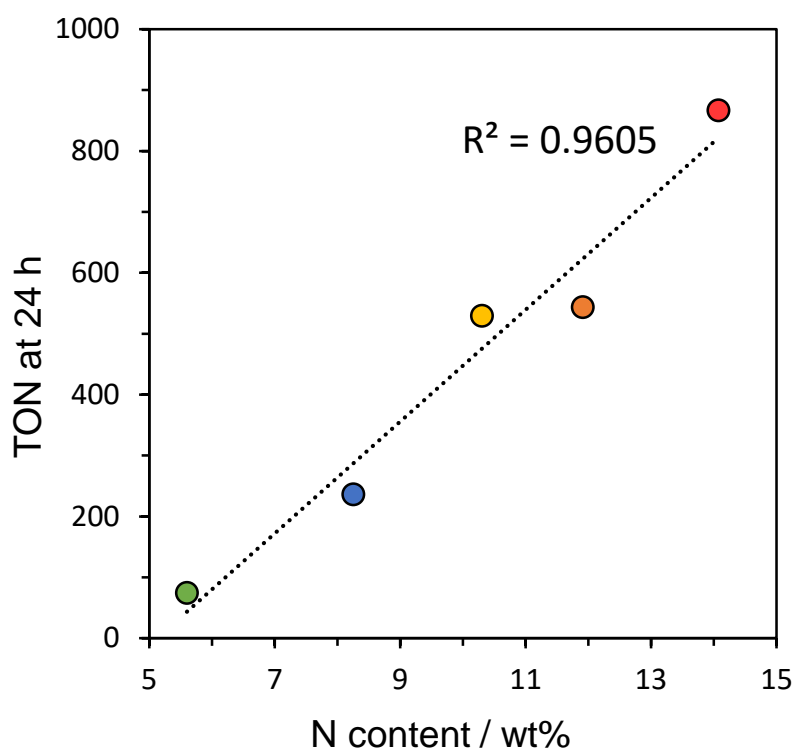


Figure S18. The relationship between TON values and total nitrogen content of each catalysts.

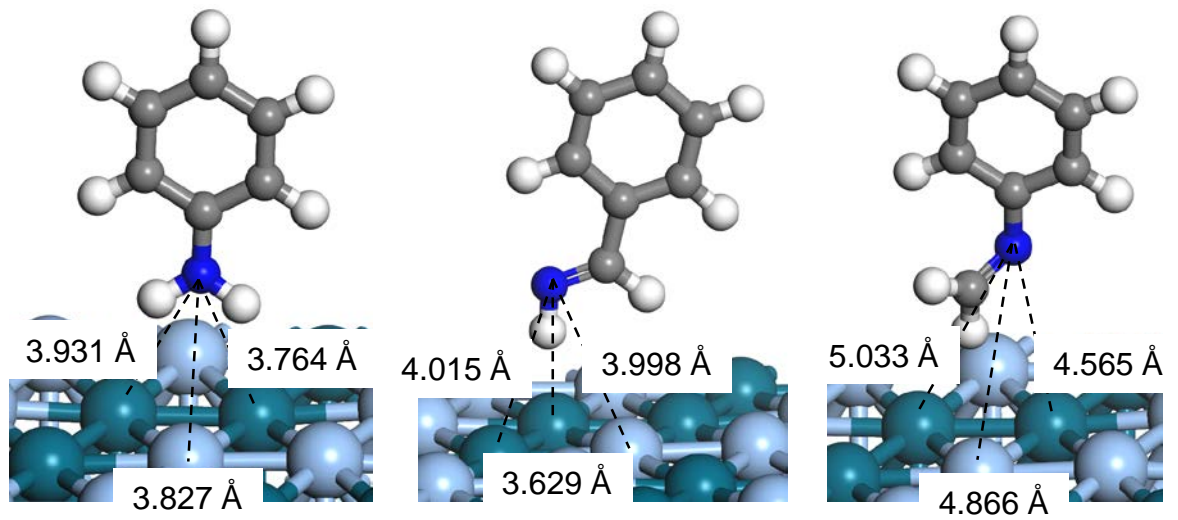


Figure S19. Adsorption state of (a) phenylamine, (b) Phenylmethanimine and (c) phenylimine on the surface of PdAg alloy model in the DFT calculations.

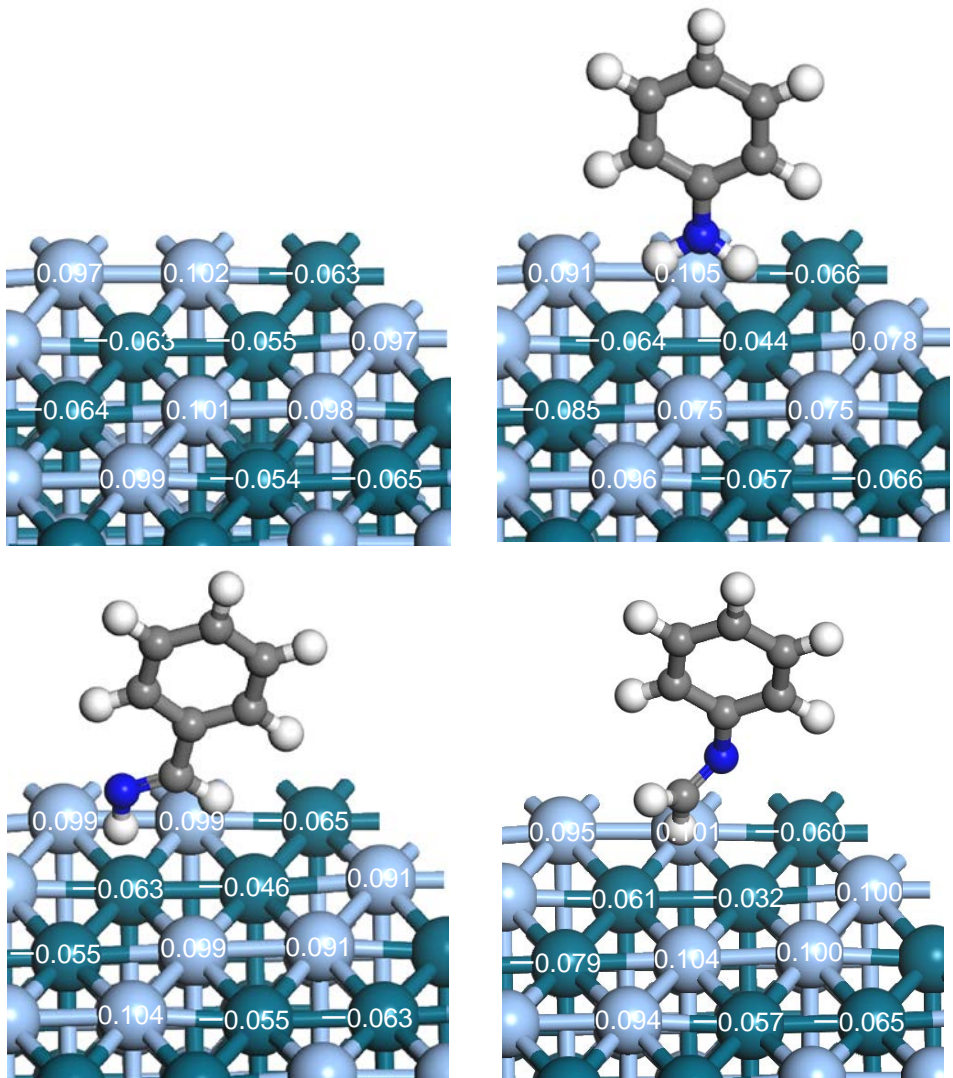


Figure S20. Difference of mulliken atomic charge of Pd and Ag atoms (a) on the pure PdAg model in the presence of (b) phenylamine, (c) phenylmethanimine and (d) phenylimine moieties.

Table S1. CO adsorption property and Pd loading amount of PdAg/amine-RF10.

sample	CO adsorbed amount [mL·g ⁻¹ (50 °C)]	Average diameter (CO adsorption) [nm]	Dispersion [%]	Pd loading amount (ICP) [wt%]
PdAg/amineRF10	0.032	73.5	1.5	1.00

Table S2. Comparison of the activity in the transformation of CO₂ to FA in the pure water condition.

	Time [h]	Pressure(H ₂ /CO ₂)	TON	TOF [h ⁻¹]	Reference
PdAg/amine-RF10	24	20/20 [MPa]	63	2.6	This work
PdNi/CNT	16	25/25 [bar]	3	0.2	[1]
0.6Pd/g-C ₃ N ₄	16	25/25 [bar]	24	1.5	[2]
2Pd/ECN	16	25/25 [MPa]	35	2.2	[3]

Solvent: water, Temperature: 40 °C

Ref. [1] Nguyen, L. T. M.; Park, H.; Banu, M.; Kim, J. Y.; Youn, D. H.; Magesh, G.; Kim, W. Y.; Lee, J. S. Catalytic CO₂ Hydrogenation to Formic Acid over Carbon Nanotube-Graphene Supported PdNi Alloy Catalysts. *RSC Adv.* 2015, 5, 105560–105566.[2] Park, H.; Lee, J. H.; Kim, E. H.; Kim, K. Y.; Choi, Y. H.; Youn, D. H.; Lee, J. S., A highly active and stable palladium catalyst on a g-C₃N₄ support for direct formic acid synthesis under neutral conditions. *Chem Commun* 2016, 52, 14302-14305.[3] Mondelli, C.; Puertolas, B.; Ackermann, M.; Chen, Z.; Perez-Ramirez, J., Enhanced Base-Free Formic Acid Production from CO₂ on Pd/g-C₃N₄ by Tuning of the Carrier Defects. *ChemSusChem* 2018, 11 (17), 2859-2869.**Table S3.** The proportion of Pd²⁺/Pd⁰ percentage observed in Pd 3d XPS analysis over each PdAg-supported catalysts.

	Pd ²⁺ / %	Pd ⁰ / %
PdAg/RF	63.9	36.1
PdAg/amine-RF3	65.8	34.2
PdAg/amine-RF5	48.7	51.3
PdAg/amine-RF7	40.3	59.7
PdAg/amine-RF10	49.9	50.1

Table S4. Comparison of CO₂ adsorption property of RF and amine-RF10 supports.

	CO ₂ adsorbed amount [mmol/g]	CO ₂ adsorption rate [mmol/g·h ⁻¹]
RF	0.10	0.40
amine-RF10	0.15	0.68